# Dynamical topological quantum phase transitions in high-order topological systems

Hai-Xiao Xiao [1], Weilun Jiang,[2,3] Peng Qian,[1] Hongju Li,[1] Zhongjun Li,[1,2,*] Heng Shen,[2,3,†] and Bing Chen [1,‡]

[1]*Department of Physics, Hefei University of Technology, Hefei, Anhui 230009, China*

[2]*State Key Laboratory of Quantum Optics and Quantum Optics Devices, Institute of Opto-Electronics,*
*Shanxi University, Taiyuan 030006, China*

[3]*Collaborative Innovation Center of Extreme Optics, Shanxi University, Taiyuan, Shanxi 030006, China*

We investigate the nonequilibrium dynamics of two multiband boundary-obstructed topological systems (BOTSs) and a higher-order topological superconductor (HOTSC). The singular behavior exhibited by the dynamical free energy indicates the presence of dynamical quantum phase transitions (DQPTs) within these systems. By studying the nonequilibrium dynamics in the BOTS featuring even-parity Cooper pairing, we find that there are DQPTs in this BOTS via quenching from different topological phase regions. The analysis of the energy spectra shows that two previously considered identical topological phases are actually different. Based on this result, we identify that all DQPTs in the BOTS featuring even-parity Cooper pairing result from topology-changing quenches. Moreover, we also study DQPTs in another BOTS featuring odd-parity Cooper pairing, and we obtain similar results to those from the BOTS featuring even-parity Cooper pairing. The appearance of DQPTs in different BOTSs reveals that the occurrence of DQPTs is related to the topology of BOTSs. In addition, we adopt the same method to investigate DQPT in HOTSC for comparison. The numerical results show that DQPT always takes place for quenches between topological and trivial phases. This is completely different from the results of BOTSs, for which not all topology-changing quenches are accompanied by DQPTs. The study of DQPTs unveils the apparent difference between BOTS and HOTSC, and thus our study provides an alternative approach to revealing the topological nature of novel higher-order topological systems, which does not rely on the specific definitions of topological invariants.

## I. INTRODUCTION

Discoveries of topological insulators and the quantum Hall effect have boosted the exploration of novel topological phases of matter [1,2]. In contrast to the conventional Landau paradigm of local order parameters, topological quantum states are characterized by nonlocal invariants that are constrained to take integer values, such as Chern numbers [3–5]. Thus, a transition between distinct topological phases is accompanied by a discontinuous change in such integer values [6]. While the behavior of equilibrium systems is well established, nontrivial band-structure topology and the associated topological phenomena in far-from-equilibrium conditions have only recently begun to be explored [7–9].

In parallel, the concept of a dynamical quantum phase transition (DQPT), featuring physical quantities that become nonanalytic as a function of real time, was recently proposed to understand the general properties of nonequilibrium quantum states [10–14], and it has been observed experimentally in several platforms [15–18]. In a DQPT, the complex Loschmidt amplitude $\mathcal{G}(t)$ plays the role of the partition function $Z = \text{Tr}[e^{-H/k_B T}]$ in equilibrium [19,20], with $H$ being the system Hamiltonian, $T$ the temperature, and $k_B$ the Boltzmann constant. The associated counterpart to the free-energy density is defined as $\Lambda(t) = -\frac{1}{N}\log[\mathcal{G}(t)]$, which behaves nonanalytically at the critical time $t_c$ in the thermodynamic limit [19–21] as a consequence of the emergence of dynamic Fisher zeros. Pioneering theoretical works have suggested a connection between DQPTs and emergent topological phenomena in nonequilibrium dynamics [22–30]. It has been found that topology-changing quenches in a variety of one-dimensional (1D) and two-dimensional (2D) systems, such as the Su-Schrieffer-Heeger (SSH) model and the Haldane model, are always followed by DQPT [31–34]. Importantly, the dynamical topological order parameter, a dynamical analog of a topological order parameter, was introduced to capture the geometric origin of DQPT [25,33]. In particular, dynamical topological order parameters (DTOPs) can only change their integer values when DQPTs occur, offering the possibility to dynamically monitor the topology change of the underlying Hamiltonian during the quench. The corresponding experimental simulation has been implemented by using 1D discrete-time quantum walks of single photons [35].

Specifically, most of the existing works fall into the category of conventional topological phases with well-defined topological invariants for the bulk, and they exhibit bulk gap closings at transition points. In fact, several exotic topological phases have recently been reported whose bulk states cannot be assigned well-defined topological invariants [36–39]. A

*Contact author: zjli@hfut.edu.cn

†Contact author: hengshen@sxu.edu.cn

‡Contact author: bingchenphysics@hfut.edu.cn

universal and robust characterization of topological DQPTs has to be applicable to such unconventional topological systems, but this has yet to be unveiled.

We have studied DQPTs in the quench dynamics of two four-band boundary-obstructed topological systems (BOTSs). Boundary-obstructed topological insulators have been proposed as a class of higher-order topological insulators (TIs) to support robust lower-dimensional boundary signatures without being associated with a bulk invariant [38–43]. Beyond standard symmetry-protected band topology, boundary-obstructed band topology can be changed without bulk closure, but it features a closed surface (edge) band gap at the phase transition point instead. It has been pointed out in previous studies that the edge topology of a BOTS ultimately comes from bulk properties, but the topological corner states are not protected by the bulk Hamiltonian [38], and the BOTS has been classified as an edge-corner correspondence type [37]. Studying the nonequilibrium dynamics in a BOTS can extend our understanding of the relationship between topology and out-of-equilibrium dynamics. By performing quantum simulations, we find that there are DQPTs in the BOTS featuring even-parity Cooper pairing, and the conventionally defined DTOPs are not exactly quantized regardless of whether a DQPT occurs or not. After thoroughly studying the definition of the DTOP, we find that it is ill-defined in a BOTS and uncorrelated with the topological property, thus it cannot be regarded as an order parameter. Furthermore, we have studied the energy spectra of this BOTS, and we found that two topological phases that were previously considered identical are actually different. Based on this result, we discovered that all DQPTs in the BOTS featuring even-parity Cooper pairing originate from topology-changing quenches, but not all topology-changing quenches are accompanied by DQPTs. This leads to the observation that the phase diagram of the DQPT is not exactly in accordance with the topological phase diagram of this BOTS. To examine whether the DQPTs in the BOTS featuring even-parity Cooper pairing are accidental or model-dependent, we have also studied the nonequilibrium dynamics in another BOTS featuring odd-parity Cooper pairing. We obtained similar results: (i) There are DQPTs in the BOTS featuring odd-parity Cooper pairing that all result from topology-changing quenches; and (ii) the phase diagram of the DQPT is not completely in accordance with the topological phase diagram. These results indicate that the appearance of DQPTs in a BOTS is related to the topology of the BOTS. In comparison, we have also studied DQPTs in a higher-order topological superconductor (HOTSC), in which the topological corner states have been proven to be protected by bulk symmetry [38]. We find that quenches between the topological phase and the trivial phase are always accompanied by DQPTs. These results reveal an apparent difference between a BOTS and a HOTSC. Therefore, we conclude that our method may be implemented as a ubiquitous tool to distinguish the topological phases of the initial and final Hamiltonian in the quench dynamics.

## II. MODEL AND METHODS

The Hamiltonian of the boundary-obstructed system featuring even-parity Cooper pairing [37] studied in this paper is given by

$$\hat{H} = \sum_{\mathbf{k}} \hat{\psi}_{\mathbf{k}}^{\dagger} H(\mathbf{k}) \hat{\psi}_{\mathbf{k}}, \tag{1}$$

where $\hat{\psi}_{\mathbf{k}} = (c_{a,\mathbf{k}}, c_{b,\mathbf{k}}, c_{a,-\mathbf{k}}^{\dagger}, c_{b,-\mathbf{k}}^{\dagger})$, and $H(\mathbf{k})$ has the following form:

$$H(\mathbf{k}) = M(\mathbf{k})\sigma_z \tau_z + \lambda_x \sin k_x \sigma_x \tau_z + \lambda_y \sin k_y \sigma_y \tau_z + \Delta \tau_x, \tag{2}$$

where $M(\mathbf{k}) = t_x \cos k_x + t_y \cos k_y - \mu$. Pauli matrices $\sigma_i$ and $\tau_i$ act in the orbital $(a,b)$ and particle-hole spaces, respectively, $t_{x,y}(\lambda_{x,y})$ are the hopping strength and spin-orbit interactions, $\Delta$ represents the pairing strength, and $\mu$ is the chemical potential.

The Hamiltonian of Eq. (2) has chiral symmetry $\mathbf{\Pi}$, time-reversal symmetry $\mathbf{\Theta}$, and particle-hole symmetry $\mathbf{\Xi}$. According to the tenfold classification [44], the system belongs to the BDI class in two dimensions. Moreover, in this system all sorts of mirror symmetry and the $C_4$ rotation symmetry are absent [28,45]. Thus the bulk state cannot be assigned a topological invariant in the conventional way.

By diagonalizing $H(\mathbf{k})$, we can obtain the four energy bands,

$$\epsilon_{1,k} = \epsilon_{2,k} = -\sqrt{M(\mathbf{k})^2 + \Delta^2 + \lambda_x^2 \sin^2 k_x + \lambda_y^2 \sin^2 k_y},$$

$$\epsilon_{3,k} = \epsilon_{4,k} = \sqrt{M(\mathbf{k})^2 + \Delta^2 + \lambda_x^2 \sin^2 k_x + \lambda_y^2 \sin^2 k_y}. \tag{3}$$

As we can see, the upper two bands and the lower two bands are degenerate separately, and the quasiparticle Hamiltonian can be rewritten as $\hat{H} = \sum_{i=1}^4 \sum_{\mathbf{k}} \epsilon_{i,k} b_{i,\mathbf{k}}^{\dagger} b_{i,\mathbf{k}}$, where $b_{i,k}$ and $b_{i,k}^{\dagger}$ are linear combinations of $c_{a(b),\mathbf{k}}$ and $c_{a(b),\mathbf{k}}^{\dagger}$. The ground state of the system is $|\psi^0\rangle = \Pi_{\mathbf{k}}|\psi_{\mathbf{k}}^0\rangle = \Pi_{\mathbf{k}} b_{2,\mathbf{k}}^{\dagger} b_{1,\mathbf{k}}^{\dagger}|\text{vac}\rangle$, where $|\text{vac}\rangle$ is the Bogoliubov vacuum with $b_{i,k}|\text{vac}\rangle = 0$. Since the Hamiltonian conserves the parity of the particle number, we can rewrite the Hamiltonian in a new basis. The details are given in the Supplemental Material (SM) [46]. Finally, we get another expression of $|\psi_{\mathbf{k}}^0\rangle$,

$$\left|\psi_{\mathbf{k}}^0\right\rangle = |\Psi_{1,\mathbf{k}}\rangle = \sum_{i=1}^6 Q_i(\mathbf{k})|\varphi_{i,\mathbf{k}}\rangle, \tag{4}$$

where $|\varphi_{i,\mathbf{k}}\rangle$ are even-parity fermion states; see the definitions in the SM [46]. $Q_i(\mathbf{k})$ are the corresponding coefficients.

In this paper, we adopt the same choice as in Ref. [37] by choosing $\Delta = \Delta_0 + \Delta_x \cos k_x + \Delta_y \cos k_y$, with $\Delta_x = -\Delta_y = \Delta_d$, where $\Delta_0$ and $\Delta_d$ are the gap parameters due to the $s$-wave and $d$-wave pairings. Moreover, we set $t_x = t_y = \lambda_x = \lambda_y = \mu = t$, $\Delta_0 = 0.5t$, and we regard $\Delta_d$ as the sole tuning parameter, just as in Fig. 1(a).

## III. OBSERVABLES

To explore such quench dynamics with respect to topological properties, we adopt two sorts of observables, i.e., the Loschmidt amplitude (LA) and DTOPs [25,33], to capture the emergent geometric structure of the quench dynamics. In the following, we give definitions for LA and DTOPs and primary derivations based on the Hamiltonian in Eq. (2).

In Fig. 1(b), we give the energy spectrum of the current model. As illustrated in Ref. [37], the appearance of the zero-
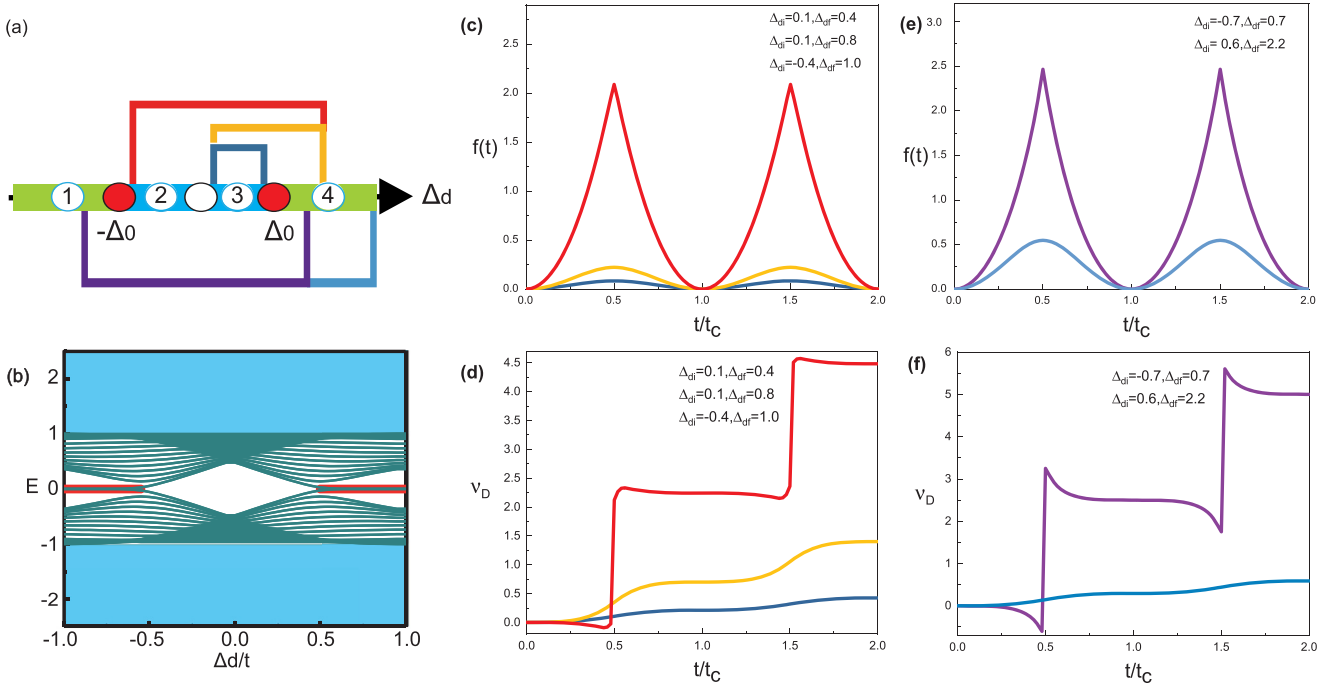
FIG. 1. (a) The topological phase diagram of the BOTS featuring even-parity Cooper pairing. For $|\Delta_d| > |\Delta_0|$, the system is in a topological phase (green). For $0 \leqslant |\Delta_d| < |\Delta_0|$, the system is in a trivial phase (blue). (b) The spectrum of the boundary-obstructed model in a square geometry with size in each direction, $N = 32$. The blue lines and the dark cyan lines show the bulk gap and the edge gap, respectively. The red line represents the zero-energy edge states. (c) and (e) The rate function $f(t)$ as a function of time for various quantum quenches. (d) and (f) The DTOP $\nu_D(t)$ as a function of time for different quantum quenches. Here, (c) and (d) take the same quench parameters, and (e) and (f) take the same quench parameters.

energy corner states is taken as the criterion for a topological phase transition in BOTS, and the system will experience a topological phase transition from a trivial state to a topological phase by varying the value of $\Delta_d$. In the current work, we denote $\Delta_{di}$ as the $d$-wave superconducting amplitude for the initial state, and $\Delta_{df}$ as the $d$-wave superconducting amplitude for the postquench Hamiltonian. First, we prepare the system in its ground state, $|\psi^0(\Delta_{di})\rangle$, then we quench the initial ground state with the Hamiltonian $\hat{H}^f(\Delta_{df})$. In this case, LA is written as

$$
\begin{aligned}
\mathcal{L}(\Delta_{di}, \Delta_{df}, t) &= \langle\psi^0(\Delta_{di})|e^{-i\hat{H}^f t}|\psi^0(\Delta_{di})\rangle \\
&= \prod_{\mathbf{k}} \mathcal{L}_{\mathbf{k}}(\Delta_{di}, \Delta_{df}, t) \\
&= \prod_{\mathbf{k}} \langle\psi_{\mathbf{k}}^0(\Delta_{di})|e^{i\hat{H}^f t}|\psi_{\mathbf{k}}^0(\Delta_{di})\rangle.
\end{aligned} \quad (5)
$$

Expanding $|\psi^0(\Delta_{di})\rangle = \sum_{i=1}^{6} a_i |\Psi_{i,\mathbf{k}}^f\rangle$, where $|\Psi_{i,\mathbf{k}}^f\rangle$ is the eigenfunction of $\hat{H}^f$ and $a_i$ is the coefficient, we can obtain the analytical expression of LA in the $\mathbf{k}$ sector,

$$
\begin{aligned}
\mathcal{L}_{\mathbf{k}}(\Delta_{di}, \Delta_{df}, t) &= (a_1^2 + a_6^2)\big[\cos\big(\varepsilon_{1,k}^f t\big) - 1\big] \\
&\quad + 1 - i\sin\big(\varepsilon_{1,k}^f t\big)(a_1^2 - a_6^2),
\end{aligned} \quad (6)
$$

where $\varepsilon_{1,k}^f$ is the lowest eigenenergy of $\hat{H}^f$, and a detailed derivation is given in the SM [46].

The rate function of LA is defined as

$$
f(t) = -\frac{1}{N}\sum_{\mathbf{k}} \ln |\mathcal{L}_{\mathbf{k}}(\Delta_{di}, \Delta_{df}, t)|^2, \quad (7)
$$

where the singularity of the rate function signals the DQPT.

Furthermore, LA can be expressed as $\mathcal{L}_{\mathbf{k}} = |\mathcal{L}_{\mathbf{k}}|e^{i\phi_{\mathbf{k}}(t)}$, and the Pancharatnam geometric phase (PGP) [25] can be obtained $\phi_{\mathbf{k}}^G(t) = \phi_{\mathbf{k}}(t) - \phi_{\mathbf{k}}^D(t)$, where $\phi_{\mathbf{k}}^D(t) = -\int_0^t ds \langle\Psi_{0,\mathbf{k}}(s)|\hat{H}|\Psi_{0,\mathbf{k}}(s)\rangle$ is the dynamical phase. Utilizing the geometric phase, one can define the DTOP in two dimensions [33],

$$
\nu_D(t) = \frac{1}{2\pi}\int_0^\pi dk_x \frac{\partial}{\partial k_x}\left[\int_0^\pi dk_y \frac{\partial\phi_{\mathbf{k}}^G}{\partial k_y}\right]. \quad (8)
$$

DTOPs are put forward as the integer-quantized winding number of $\phi_{\mathbf{k}}^G(t)$ over the effective Brillouin zone (EBZ) to characterize the emergence of a topological structure associated with the temporal evolution of quench systems in one and two dimensions [25,33]. When the DTOP shows a quantized change, it indicates the emergence of topological structure during the quantum quench process. In the following context, we calculate LA and DTOPs for both BOTS and HOTSC.

## IV. DQPTS AND TOPOLOGICAL PHASE DIAGRAM IN THE BOTS FEATURING EVEN-PARITY COOPER PAIRING

Within this section, we delineate the quench dynamics framework and present the numerical findings in the BOTS featuring even-parity Cooper pairing.

We simulate several quenches with different values of $\Delta_{di}$ and $\Delta_{df}$. The results for LA and DTOPs are shown in Figs. 1(c)–1(f). As we can see from Figs. 1(c) and 1(e), DQPTs occur for $\Delta_{di} = -0.4t$, $\Delta_{df} = 1.0t$ and $\Delta_{di} = -0.7t$,

$\Delta_{df} = 0.7t$. The critical times for DQPTs are

$$t_n^* = (2n+1)t_c, \quad t_c = \frac{-\pi}{\varepsilon_{1,k}^f(\Delta_{df})}, \quad n \in \mathbb{Z}. \quad (9)$$

These results indicate that DQPTs appear in this BOTS when quench starts from the bulk states.

Utilizing the geometric phase obtained from LA, we have also computed the DTOPs for these quenches. From Figs. 1(d) and 1(f), we find that DTOP varies continuously and remains nonzero when DQPT does not occur. Beyond that, it shows rapid variation at the critical time when DQPTs take place. Meanwhile, the plateau magnitudes of the DTOP are not integer. Such characteristics of the DTOP can be understood by referring to discussions given in Refs. [25] and [33]. The DTOP is well defined when the PGP is defined on momentum intervals, which are able to form closed circles [25,33]. This condition is ensured by the existence of paired fixed points [25,28,31,35,47]. However, in the BOTS featuring even-parity Cooper pairing, as we have shown in the SM [46], such paired fixed points do not exist, and the DTOPs are always noninteger. This leads to the conclusion that the DTOP is ill-defined in the BOTS and does not represent a topological property of the quench dynamics.

To further explore the conditions for the DQPTs to occur in this BOTS, we also study the phase diagram of DQPT. When the real and imaginary parts of $\mathcal{L}_\mathbf{k}(\Delta_{di}, \Delta_{df}, t)$ in Eq. (6) are both equal to zero, the rate function will show singular behavior at a critical time $t_n^*$. Then, we further obtain the phase diagram of DQPT in $\Delta_{di}$ and $\Delta_{df}$ space for the BOTS featuring even-parity Cooper pairing, as shown in Fig. 2(a). For different initial and final states in Fig. 1(a), there are 16 kinds of quench schemes in total, and they are marked with different numbers in Fig. 2(a). As we can see, for areas all covered in blue, like 11,22,23,32,33,44, there are no DQPTs. This shows that quenches among the same topological phase are not accompanied by DQPTs.

Moreover, for quenches among part 1(4) and part 4(1) of Fig. 1(a), DQPTs always take place. To understand these results, we plot the edge states of the BOTS featuring even-parity Cooper pairing for different phases in Fig. 3. As we can see, for $\Delta_d < -0.5t$, there are two isolated in-gap edge states only in the $y$-direction. The edge states in the $x$-direction are trivial. However, for $\Delta_d > 0.5t$, there are two isolated in-gap edge states in the $x$-direction. The edge states in the $y$-direction are trivial. The appearance of topologically protected in-gap edge states reveals the nontrivial topological property of the system [48]. Previous studies have shown that in an anisotropic system, such topological edge states only appear in one direction, and the in-gap edge states appear in different directions corresponding to different topological phases [48]. The same arguments apply to the current model. Therefore, the topological phases in parts 1 and 4 of Fig. 1(a) are different. This result indicates that DQPTs appearing in areas, i.e., 14 and 41 in Fig. 2(a), result from topology-changing quenches. As a result, we distinguish these two topological phases in Fig. 2(b), which are covered by different colors. Furthermore, these topological states can be characterized by a two-component topological invariant $(\Gamma_x, \Gamma_y)$, where $\Gamma_x, \Gamma_y$ are topological numbers defined for the edge states in Ref. [37].
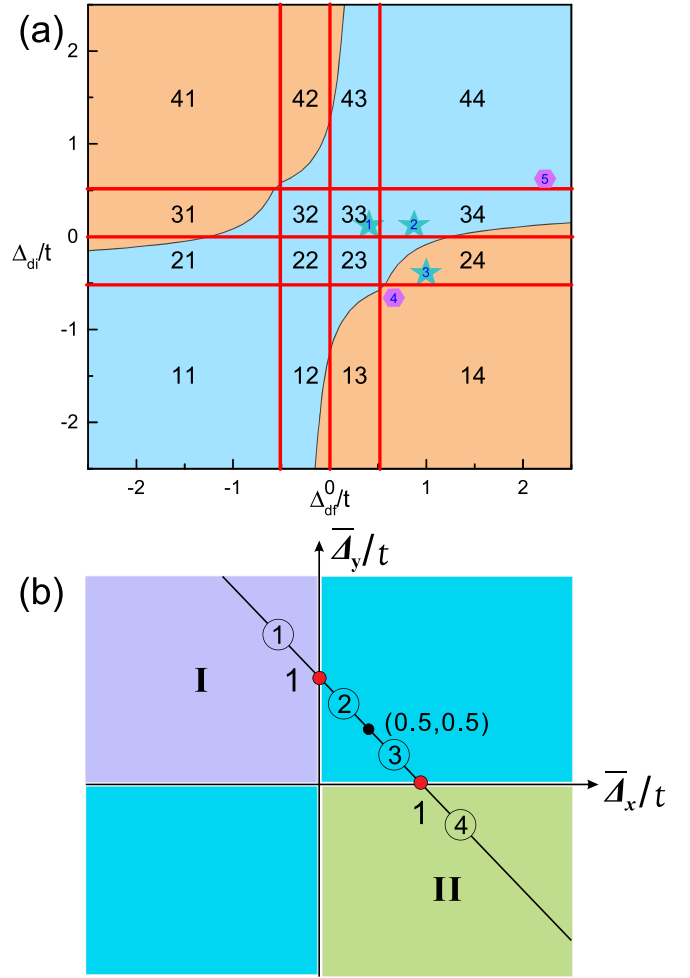


FIG. 2. (a) The phase diagram of DQPTs in $\Delta_{di}$ and $\Delta_{df}$ space. The numbers in the phase diagram, for example $ij$, indicate that in this area, $\Delta_{di}$ belongs to the $i$th part of the phase diagram in Fig. 1(a), and $\Delta_{df}$ belongs to the $j$th part of the phase diagram in Fig. 1(a). In the dark yellow (blue) areas, quenches will (will not) lead to DQPTs. The star (hexagon) symbols with numbers represent quenches in Figs. 1(c) and 1(e), with the numbers representing the order of these quenches as they appear in the legend. (b) The topological phase diagram of the boundary-obstructed model in $\bar{\Delta}_x$ and $\bar{\Delta}_y$ space, with $\bar{\Delta}_{x,y} = \Delta_0 + (\mu - t_x - t_y)\Delta_{x,y}/t_{x,y}$. Phases in the purple and green areas are topological phases, labeled I and II. Conversely, phases in blue areas are trivial phases. In this paper, we focus on the $d$-wave pairing case, in which $\Delta_x = -\Delta_y = \Delta_d$. All considered states are located on the black solid line, and they are divided into four parts, corresponding to Fig. 1(a).

For other quench schemes in Fig. 2(a), represented by areas 12,13,21,24,31,34,42,43, DQPTs do not always occur. These quenches are among trivial states and topological nontrivial states.

## V. DQPTS IN ANOTHER BOUNDARY-OBSTRUCTED TOPOLOGICAL SYSTEM WITH ODD-PARITY COOPER PAIRING

To further examine whether the DQPTs that appear in the BOTS featuring even-parity Cooper pairing are accidental or model-dependent, we study the quench dynamics in another
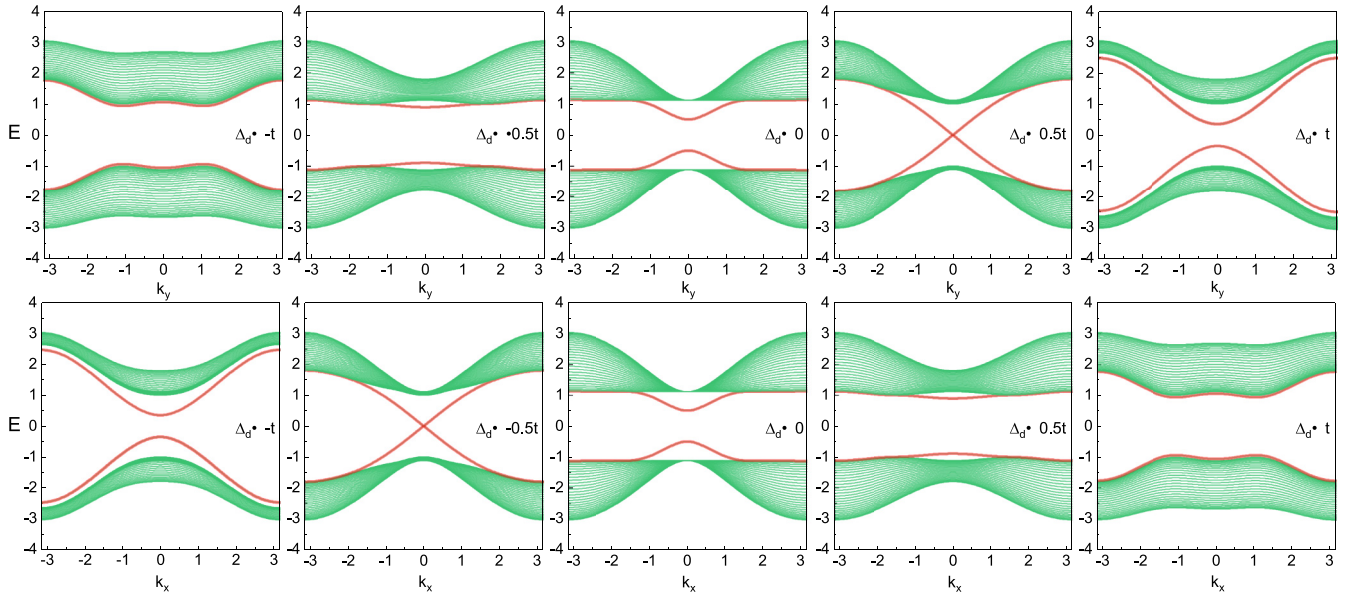
FIG. 3. Energy spectra of the BOTS featuring even-parity Cooper pairing under different open boundary conditions for different $\Delta_d$. The five spectra in the upper panels are obtained with the periodic boundary condition in the $y$-direction and the open boundary condition in the $x$-direction. The five spectra in the lower panels are obtained with the periodic boundary condition in the $x$-direction and the open boundary condition in the $y$-direction.

BOTS featuring odd-parity Cooper pairing proposed in previous work [38]. In Ref. [38], the authors proposed a model

$$H = t(\cos k_x + \gamma_x)\sigma_x\tau_z + t(\cos k_y + \gamma_y)\sigma_z\tau_z$$
$$+ \Delta \sin k_x \tau_x + \Delta \sin k_y \tau_y, \quad (10)$$

where $t$ is the hopping amplitude, $\Delta$ is the superconducting gap, $\gamma_x$ and $\gamma_y$ are the tuning parameters, $\sigma_\mu$ acts within the subspace of the normal state bands, and $\tau_\nu$ acts on the Nambu space indices, with $\mu, \nu = x, y, z$. The topological bulk-boundary correspondence of this model is completely contingent upon the low-energy description of the normal state [38]. Without loss of generality, we take $\Delta = 0.4t$ and $t = 1$ in this paper. When $\gamma_y = 0(\gamma_x = 0)$ and $\gamma_x \neq 0(\gamma_y \neq 0)$, the $C_4$ rotation symmetry of this model is broken, and it describes a boundary-obstructed topological system with $C_2$ rotation symmetry. Here, we choose $\gamma_y = 0, \gamma_x \neq 0$. As shown in Fig. 4(e), for $0 < \gamma_x < 1$ the system is topological with zero-energy topological corner states; for $\gamma_x > 1$ the system is in a trivial state.

By taking different quantum quenches, we obtain the rate functions for these quenches, and the results are presented in Fig. 4(a). As we can see, there are also DQPTs in the BOTS featuring odd-parity Cooper pairing. Moreover, we obtain the phase diagram of DQPTs in the BOTS featuring odd-parity Cooper pairing. This phase diagram is similar to the DQPT phase diagram in Fig. 2(a). All DQPTs in this system result from topology-changing quenches, while not all topology-changing quenches are accompanied by DQPTs. Furthermore, we provide the energy spectrum of two different states of the BOTS featuring odd-parity Cooper pairing with certain boundary conditions. The energy spectrum in Fig. 4(c) [4(d)] is in the topological (trivial) state, and it manifests (does not manifest) in gap edge states.

## VI. DQPTS IN A HIGH-ORDER TOPOLOGICAL SUPERCONDUCTOR

In this section, we use the same method to study the DQPTs in a 2D HOTSC. The model of the 2D HOTSC can be obtained by setting $\gamma_x = \gamma_y = \gamma$ in Eq. (10), which gives

$$H = t(\cos k_x + \gamma)\sigma_x\tau_z + t(\cos k_y + \gamma)\sigma_z\tau_z$$
$$+ \Delta \sin k_x \tau_x + \Delta \sin k_y \tau_y. \quad (11)$$

When $0 < \gamma < 1$, the normal state has four Dirac points, and such a model describes a 2D HOTSC with corner Majorana modes; when $\gamma > 1$, no Dirac point exists, and this Hamiltonian describes a trivial $p + ip$-wave superconductor without corner Majorana modes. As a result, by changing the value of $\gamma$, we can turn the system from a topological phase to a trivial phase.

After adopting quantum simulations, we obtained the numerical results of LA and DTOPs for several quantum quenches, as presented in Fig. 5(a). As we can see, for $\gamma_1$ and $\gamma_2$ on opposite sides of $\gamma = 1$ there are DQPTs, and the DTOP shows a discontinuous jump with the magnitude equal to two units; for $\gamma_1$ and $\gamma_2$ on the same side of $\gamma = 1$, DQPTs are absent and the DTOPs are continuous. Furthermore, we obtain the phase diagram of DQPTs of this model, and the result is shown in Fig. 5(b). The regions where DQPTs occur have clear phase boundaries at $\gamma_1 = 1$ and $\gamma_2 = 1$. These phase boundaries are fully consistent with the topological phase transition boundary of the HOTSC, indicating that the topological property of the HOTSC is completely determined by the bulk Hamiltonian.

## VII. SUMMARY AND DISCUSSION

The relation between topology and nonequilibrium dynamics has been widely studied. While previous studies focused
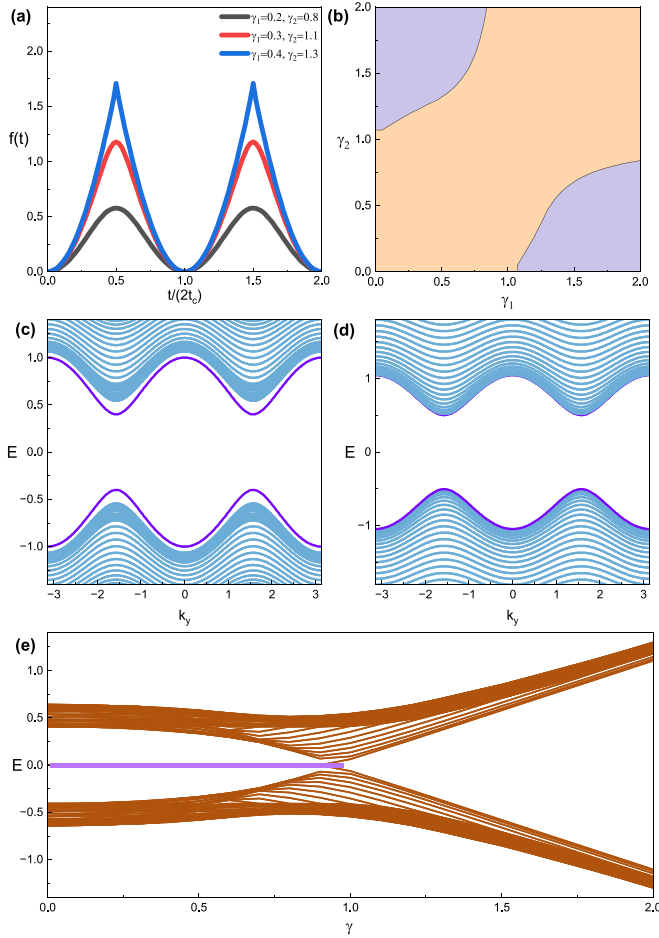
FIG. 4. (a) The rate function $f(t)$ in another BOTS featuring odd-parity Cooper pairing, proposed in Eq. (10), for three different quantum quenches: $\gamma_1 = 0.2, \gamma_2 = 0.8$; $\gamma_1 = 0.3, \gamma_2 = 1.1$; and $\gamma_1 = 0.4, \gamma_2 = 1.3$. Here we denote $\gamma_1$ as the prequench value of $\gamma_x$, and $\gamma_2$ as the postquench value of $\gamma_x$. (b) The phase diagram of DQPTs in $\gamma_1$ and $\gamma_2$ space for the BOTS featuring odd-parity Cooper pairing. The purple (dark yellow) areas indicate that quenches in this area will (will not) cause DQPTs in the BOTS featuring odd-parity Cooper pairing. (c) The energy spectrum of the BOTS featuring odd-parity Cooper pairing for $\gamma_x = 0.4$ and 1.3, with the periodic boundary condition in the $x$-direction and the open boundary condition in the $y$-direction. (d) The spectrum of the boundary-obstructed model in a square geometry with size at each direction, $N = 32$, and the purple line represents the zero-energy edge states.

mainly on the correlation between the appearance of singularities in dynamical free energy and the topological invariants defined for bulk states [26,34], it is generally accepted that for a topological system with well-defined topological invariants for bulk states, topology-changing quenches are always accompanied by DQPTs. The relation between topology and nonequilibrium dynamics has rarely been explored beyond this scope. In this paper, we have studied DQPTs in two classes of higher-order topological systems, i.e., BOTS and HOTSC. First, we studied the nonequilibrium dynamics in BOTS featuring even-parity Cooper pairing, and we found that there are DQPTs in this BOTS, but the conventionally
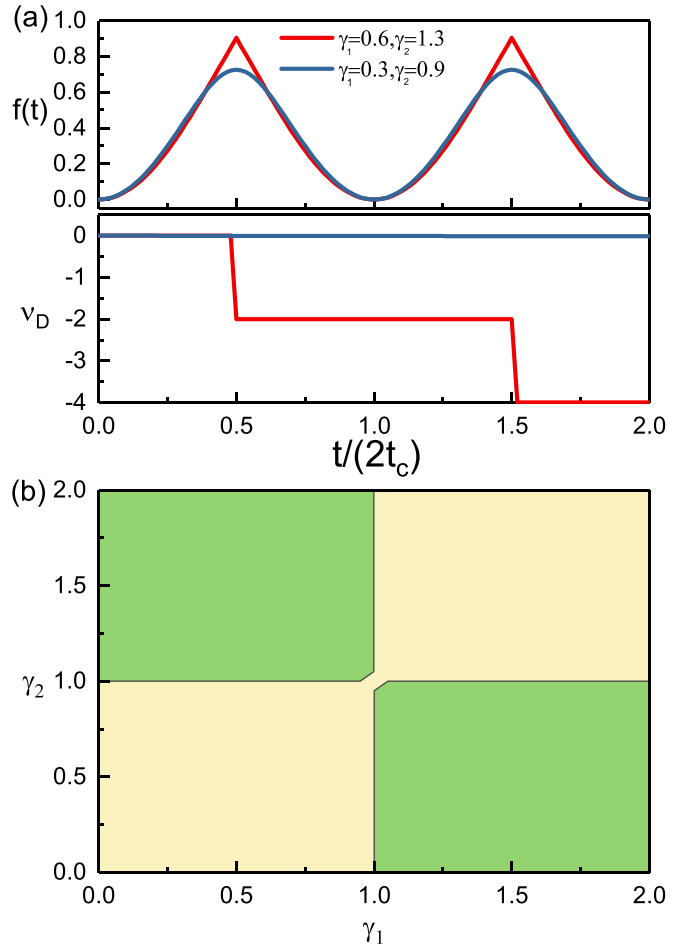
FIG. 5. (a) The rate function $f(t)$ and DTOP $\nu_D(t)$ as a function of time for various quantum quenches with $\Delta = 0.8t$. (b) The phase diagram of DQPTs in $\gamma_1$ and $\gamma_2$ space for the 2D HOTSC. Here we denote $\gamma_1$ as the prequench value of $\gamma$, and $\gamma_2$ as the postquench value of $\gamma$. The green (yellow) areas indicate that quenches in this area will (will not) cause DQPTs in the HOTSC.

defined DTOPs are not quantized for all quantum quenches. The analysis of PGP shows that the DTOP is ill-defined for BOTS, and it does not represent a topological property. To clarify the origin of DQPTs in this BOTS, we also studied the energy spectra of the BOTS with different boundary conditions, and we identified that two topological phases that were previously considered identical [37] are actually topologically distinct. To examine whether the appearance of DQPTs in the BOTS featuring even-parity Cooper pairing is accidental or model-dependent, we also studied the quench dynamics in another BOTS featuring odd-parity Cooper pairing, and we obtained similar results. The occurrence of DQPTs in different BOTS, and the fact that all DQPTs result from topology-changing quenches, reveal that the nonequilibrium dynamics is related to the topology of the BOTS. Moreover, the phase diagram of DQPTs is not in full accordance with the topological phase diagram of BOTSs. As a comparison, we also study DQPTs in a 2D HOTSC. The results show that topology-changing quenches are always accompanied by DQPTs, and the phase boundary

of DQPTs is fully in accordance with the topological phase transition boundary. Previous study [38] has shown that the topology of a 2D HOTSC is protected by the bulk Hamiltonian. Starting from the bulk Hamiltonian, our study of nonequilibrium dynamics shows clear differences between the BOTS and HOTSC.

With regard to the future, an increasing number of higher-order topological systems are being explored, but for a notable number of them, a topological invariant cannot be identified that accurately captures the topological nature of the system in a conventional way [37,38,49]; this makes it quite challenging to reveal their topological nature. Importantly, our approach does not depend on specific definitions of topological invariants, and it may offer an alternative route to under-stand the topological nature of novel higher-order topological insulators.

[1] M. Z. Hasan and C. L. Kane, Rev. Mod. Phys. **82**, 3045 (2010).

[2] X.-L. Qi and S.-C. Zhang, Rev. Mod. Phys. **83**, 1057 (2011).

[3] C.-K. Chiu, J. C. Y. Teo, A. P. Schnyder, and S. Ryu, Rev. Mod. Phys. **88**, 035005 (2016).

[4] Y. Ando and L. Fu, Annu. Rev. Condens. Matter Phys. **6**, 361 (2015).

[5] N. Goldman, J. C. Budich, and P. Zoller, Nat. Phys. **12**, 639 (2016).

[6] A. Kitaev, *Periodic Table for Topological Insulators and Superconductors*, AIP Conf. Proc. No. 1134 (AIP, Melville, NY, 2009), p. 22.

[7] M. Heyl, A. Polkovnikov, and S. Kehrein, Phys. Rev. Lett. **110**, 135704 (2013).

[8] L.-W. Zhou and J.-B. Gong, Phys. Rev. B **98**, 205417 (2018).

[9] K. Yang, L.-W. Zhou, W.-C. Ma, X. Kong, P.-F. Wang, X. Qin, X. Rong, Y. Wang, F.-Z. Shi, J.-B. Gong, and J.-F. Du, Phys. Rev. B **100**, 085308 (2019).

[10] K. Yang, S.-Y. Xu, L.-W. Zhou, Z.-Y. Zhao, T.-Y. Xie, Z. Ding, W.-C. Ma, J.-B. Gong, F.-Z. Shi, and J.-F. Du, Phys. Rev. B **106**, 184106 (2022).

[11] S. Mu, L.-W. Zhou, L.-H. Li, and J.-B. Gong, Phys. Rev. B **105**, 205402 (2022).

[12] W. Jia, X.-C. Zhou, L. Zhang, L. Zhang, and X.-J. Liu, Phys. Rev. Res. **5**, L022032

[13] B. Chen, X. F. Hou, F. F. Zhou, P. Qian, H. Shen, and N. Y. Xu, Appl. Phys. Lett. **116**, 194002 (2020).

[14] B. Chen, S. Li, X. Hou, F. Ge, F. Zhou, P. Qian, F. Mei, S. Jia, N. Xu, and H. Shen, Photon. Res. **9**, 81 (2021).

[15] N. Fläschner, D. Vogel, M. Tarnowski, B. S. Rem, D.-S. Lühmann, M. Heyl, J. C. Budich, L. Mathey, K. Sengstock, and C. Weitenberg, Nat. Phys. **14**, 265 (2018).

[16] P. Jurcevic, H. Shen, P. Hauke, C. Maier, T. Brydges, C. Hempel, B. P. Lanyon, M. Heyl, R. Blatt, and C. F. Roos, Phys. Rev. Lett. **119**, 080501 (2017).

[17] J. Zhang, G. Pagano, P. W. Hess, A. Kyprianidis, P. Becker, H. Kaplan, A. V. Gorshkov, Z.-X. Gong, and C. Monroe, Nature (London) **551**, 601 (2017).

[18] X.-Y. Guo, C. Yang, Y. Zeng, Y. Peng, H.-K. Li, H. Deng, Y.-R. Jin, S. Chen, D.-N. Zheng, and H. Fan, Phys. Rev. Appl. **11**, 044080 (2019).

[19] M. Heyl, Europhys. Lett. **125**, 26001 (2019).

[20] M. Heyl, Phys. Rev. Lett. **115**, 140602 (2015).

[21] M. Sadrzadeh, R. Jafari, and A. Langari, Phys. Rev. B **103**, 144305 (2021).

[22] M. Heyl, Rep. Prog. Phys. **81**, 054001 (2018).

[23] M. Schmitt and S. Kehrein, Phys. Rev. B **92**, 075114 (2015).

[24] M. Heyl and J. C. Budich, Phys. Rev. B **96**, 180304(R) (2017).

[25] J. C. Budich and M. Heyl, Phys. Rev. B **93**, 085416 (2016).

[26] Z. Huang and A. V. Balatsky, Phys. Rev. Lett. **117**, 086802 (2016).

[27] M. S. Rudner and N. H. Lindner, Nat. Rev. Phys. **2**, 229 (2020).

[28] R. Okugawa, H. Oshiyama, and M. Ohzeki, Phys. Rev. Res. **3**, 043064 (2021).

[29] N. Sedlmayr, P. Jaeger, M. Maiti, and J. Sirker, Phys. Rev. B **97**, 064304 (2018).

[30] P. Wang and X. Gao, Phys. Rev. A **97**, 023627 (2018).

[31] X. Qiu, T.-S. Deng, G.-C. Guo, and W. Yi, Phys. Rev. A **98**, 021601(R) (2018).

[32] X. Qiu, T.-S. Deng, Y. Hu, P. Xue, and W. Yi, iScience **20**, 392 (2019).

[33] U. Bhattacharya and A. Dutta, Phys. Rev. B **96**, 014302 (2017).

[34] S. Vajna and B. Dóra, Phys. Rev. B **91**, 155127 (2015).

[35] K. Wang, X. Qiu, L. Xiao, X. Zhan, Z. Bian, W. Yi, and P. Xue, Phys. Rev. Lett. **122**, 020501 (2019).

[36] M. Ezawa, Y. Tanaka, and N. Nagaosa, Sci. Rep. **3**, 2790 (2013).

[37] M. Ezawa, Phys. Rev. B **102**, 121405(R) (2020).

[38] A. Tiwari, A. Jahin, and Y. Wang, Phys. Rev. Res. **2**, 043300 (2020).

[39] K. Asaga and T. Fukui, Phys. Rev. B **102**, 155102 (2020).

[40] X. Wu, W. A. Benalcazar, Y. Li, R. Thomale, C. X. Liu, and J. Hu, Phys. Rev. X **10**, 041014 (2020).

[41] R. Ghadimi, S. H. Lee, and B.-J. Yang, Phys. Rev. B **107**, 224511 (2023)

[42] E. Khalaf, W. A. Benalcazar, T. L. Hughes, and R. Queiroz, Phys. Rev. Res. **3**, 013239 (2021).

[43] J. Claes and T. L. Hughes, Phys. Rev. B **102**, 100203(R) (2020).

[44] A. Altland and M. R. Zirnbauer, Phys. Rev. B **55**, 1142 (1997); A. P. Schnyder, S. Ryu, A. Furusaki, and A. W. W. Ludwig, *ibid.* **78**, 195125 (2008).

[45] E. Roberts, J. Behrends, and B. Béri, Phys. Rev. B **101**, 155133 (2020).

[46] See Supplemental Material at http://link.aps.org/supplemental/10.1103/PhysRevB.110.064306 for a detailed analysis of the models.

[47] K.-Y. Cao, S. Yang, Y. Hu, and G. Yang, Phys. Rev. B **108**, 024201 (2023).

[48] H. C. Wu, L. Jin, and Z. Song, Phys. Rev. B **102**, 035145 (2020).

[49] S. Franca, J. van den Brink, and I. C. Fulga, Phys. Rev. B **98**, 201114(R) (2018).